Computers and Geotechnics 81 (2017) 360–367

Contents lists available at ScienceDirect

Computers and Geotechnics

journal homepage: www.elsevier.com/locate/compgeo

Research Paper

# Modeling pressure pipe embedded in two-layer soil by a half-plane BEM

Mehdi Panji *, Bahman Ansari

*Department of Civil Engineering, Zanjan Branch, Islamic Azad University, Zanjan, Iran*

ARTICLE INFO

*Article history:*
Received 13 March 2016
Received in revised form 6 July 2016
Accepted 20 September 2016

*Keywords:*
Half plane BEM
Lining
Two layers soil
Embedded pipe
Stress analysis

ABSTRACT

In this paper, an elastostatic half-plane boundary element method (BEM) formulation was applied to analyze the stress behavior of underground pressure pipes, embedded in two-layer soils. In the use of this method, only the boundary of pipe and interfaces were required to be discretized. In this regard, first, a computer code was prepared based on a multi-region substructuring process in the BEM scheme. Then, the efficiency and applicability of the method as well as the prepared algorithm were verified by solving some practical examples and comparing the results with those of the published works. Finally, a parametric study was done to evaluate the effect of pipe depth and determine the soil stress distribution. The studies showed that the half-plane BEM was in good agreement with the existing solutions and its capability was very favorable for elastostatic problems including semi-infinite domain. It is obvious that this method can be practically used to analyze the geotechnical underground buildings in substituting the full-plane BEM formulation.

© 2016 Elsevier Ltd. All rights reserved.

## 1. Introduction

In big cities, underground structures as well as subsurface openings have become a major requirement for resource transmission systems. In this regard, they should be designed in such a way that could be sufficiently powered against the applied loads. Therefore, it is essential for engineers to utilize appropriate method for obtaining more accurate responses. Technically speaking, there are different methods for stress analysis of the embedded pipes which include analytical, semi-analytical, experimental and numerical ones. Due to the growth of computers and computing devices, numerical methods have been increasingly considered. Common numerical methods with regard to formulation can be divided into domain and boundary methods. In domain methods, such as finite element method (FEM) and finite difference method (FDM), by discretizing domain into the smaller elements and writing equilibrium equations for each element, the initial unknowns can be determined. Several researchers have tried to use them for analyzing geotechnical problems (Mroueh and Shahrour [18], Augarde and Burd [1] and Garner and Coffman [19]).

Although the domain methods have good accuracy for analyzing the closed media, they are not favorable for modeling infinite and semi-infinite spaces because of increase in elements number and consequently increase in calculation time. Hence, the area was prepared for the appearance of boundary methods, such as boundary element method (BEM). In this method, it is only required to discretize the boundary of the body. A complete review of BEM mathematics extension can be found in Cheng and Cheng [4]. In the use of BEM approaches, there are two types of formulations for modeling continuous semi-infinite domains, full-plane BEM and half-plane BEM. Discretizing all boundaries of the body in the closed loop as well as defining ground surface meshes to a distance far away from the interested zone is inevitable in the full-plane BEM models. Some studies have been done using this method for modeling the problem and obtaining the responses which include works by Crouch and Starfield [3], Yang and Sterling [27], Xiao and Carter [24], Wu et al. [25] and Panji et al. [11,12].

On other hand, half-plane BEM can be practically used. In this method, due to the use of image source approach [5] to satisfy the ground surface stress-free condition when solving equilibrium equations, it is not required to discretize smooth ground surface and only the boundaries under certain constrains need to be discretized. Additionally, it is not wanted to close the boundaries in the far field of the interested zone, so that the model is an opened domain. Several researchers developed this method and used them. The model of point load applied in the half-space first solved by Mindlin [16]. Telles and Brebbia [23] used Mindlin's approach and presented appropriate half-plane fundamental solutions for analyzing the homogeneous elastostatics problems. Ye and Sawada [26] explained numerical properties of half-plan BE analysis for 2-d

* Corresponding author at: Geotechnical Engineering Group, Department of Civil Engineering, Zanjan Branch, Islamic Azad University, Shahid Mansoori St., Moallem St., Zanjan, Iran.

*E-mail addresses:* m.panji@iauz.ac.ir (M. Panji), Bahman.ans@chmail.com (B. Ansari).

http://dx.doi.org/10.1016/j.compgeo.2016.09.006
0266-352X/© 2016 Elsevier Ltd. All rights reserved.

elastostatic problems. An elastic orthotropic half-plane BEM proposed by Dumir and Mehta [6]. Pan et al. [10] developed a half-plane BEM for analyzing anisotropic media. Dong et al. [8] used a different integral equation for modeling elastic half-plane inclusion problems. Later, Dong and Lo [7] developed a BEM scheme for analyzing elastic half-plane which contains nanoinhomogeneities. Also, in the field of dynamic problems, half-plane BEM has been developed that can be pointed out to studies of Panji et al. [13,14].

The related literature has indicated that half-plane BEM has not been used for stress analysis of layered semi-infinite domains containing lined cavities thus far. So, in this paper, the complete formulation of half-plane BEM for modeling a lined cavity in a layered soil was presented. In this regard, after developing a computer algorithm, and verifying the results using some available analytical solutions, a model of a circular pressure pipe buried in the second layer of a two-layer soil was examined and the effects of pipe depth on soil stress distribution were evaluated. Showing the simplicity of half-plane BEM compared to other numerical solutions in the modeling of embedded geotechnical buildings was the main purpose of this paper.

## 2. Half-plane BEM

### 2.1. Half-plane fundamental solutions

For extracting half-plane fundamental solutions, it is required to apply ground surface stress-free conditions when solving equilibrium equations. After solving the equilibrium equations, the half-plane fundamental solutions can be generally obtained as follows:

$$( )^{*} = ( )^{K} + ( )^{C} \tag{1}$$

where K denotes Kelvin's fundamental solution and C is the complementary part. Kelvin's fundamental solutions that are obtained by applying unit point load in an infinite domain without considering any boundary conditions can be written as follows [2,9]:

$$u_{ij}^{K} = \frac{1}{8\pi G(1-\nu)}\left[(3-4\nu)\ln\frac{1}{r}\delta_{ij} + r_{,i}r_{,j}\right] \tag{2}$$

$$p_{ij}^{K} = \frac{1}{4\pi(1-\nu)r}\left[\frac{\partial r}{\partial n}\left[(1-2\nu)\delta_{ij} + 2r_{,i}r_{,j}\right] + (1-2\nu)\left(n_i r_{,j} - n_j r_{,i}\right)\right] \tag{3}$$

where $u_{ij}^{K}$ and $p_{ij}^{K}$ are the Kelvin's displacement and tractions fields in the direction $j$ due to a unit point load in the direction $i$, respectively, G is the shear modulus, $\delta_{ij}$ is Kronecker delta and ν is the Poisson's ratio. According to Fig. 1 and by the assistance of image source approach for satisfying the stress free boundary conditions, the complementary parts of displacement fundamental solutions are presented as follows [23]:

$$u_{11}^{C} = k_d\left\{-[8(1-\nu)^2 - (3-4\nu)]\ln R + \frac{\left[(3-4\nu)R_1^2 - 2c\bar{x}\right]}{R^2} + \frac{4c\bar{x}R_1^2}{R^4}\right\} \tag{4}$$

$$u_{12}^{C} = k_d\left\{\frac{(3-4\nu)r_1 r_2}{R^2} + \frac{4c\bar{x}R_1 r_2}{R^4} - 4(1-\nu)(1-2\nu)\theta\right\} \tag{5}$$

$$u_{21}^{C} = k_d\left\{\frac{(3-4\nu)r_1 r_2}{R^2} - \frac{4c\bar{x}R_1 r_2}{R^4} + 4(1-\nu)(1-2\nu)\theta\right\} \tag{6}$$

$$u_{22}^{C} = k_d\left\{-\left[8(1-\nu)^2 - (3-4\nu)\right]\ln R + \frac{\left[(3-4\nu)r_2^2 + 2c\bar{x}\right]}{R^2} - \frac{4c\bar{x}r_2^2}{R^4}\right\} \tag{7}$$

In addition to the displacement part, for displaying the boundary integral, it is required to obtain the complementary traction fundamental solutions. Traction components can be easily calculated by multiplying stress tensor by unit normal vector as follows:

$$p_{ij}^{C} = \sigma_{jki}^{C} n_k \tag{8}$$

where $p_{ij}^{c}$ is the complementary part of traction fundamental solution, $n_k$ are the components of the normal to the boundary at point k, and $\sigma_{jki}^{c}$ are stress components in plane j in direction k due to load affecting direction i [23].

### 2.2. Boundary integral equation (BIE)

BIE for half-plane BEM is similar to full-plane BEM:

$$c_{ij}u^{i} = \int_{\Gamma} u_{ij}^{*} p_j \, d\Gamma - \int_{\Gamma} p_{ij}^{*} u_j \, d\Gamma \tag{9}$$

where $u_{ij}^{*}$ and $p_{ij}^{*}$ represent the half-plane fundamental solutions for the components of displacements and tractions and u as well as p represents scalar values of the displacement and tractions on boundary Γ, respectively. $c_{ij}$ are constant values that can be easily determined by rigid body motion effects [2,9,23]. After applying the above integrals to all boundaries, unknown displacements and tractions can be easily determined. Finally, for each internal point,

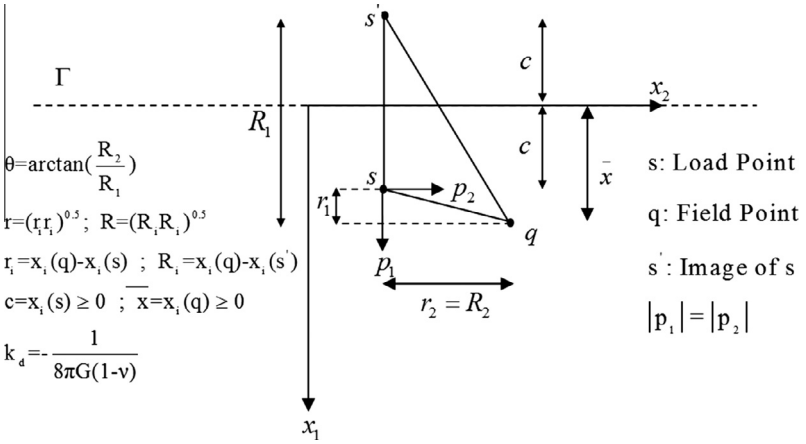


**Fig. 1.** Use of image source approach in the half-plane BEM for satisfying stress free boundary conditions [23].

the displacements and stresses can be respectively obtained using the following equations:

$$u^i = \int_\Gamma u^*_{ij} p_j \, d\Gamma - \int_\Gamma p^*_{ij} u_j \, d\Gamma \tag{10}$$

$$\sigma_{ij} = \int_\Gamma u^*_{ijk} p_k \, d\Gamma - \int_\Gamma p^*_{ijk} u_k \, d\Gamma \tag{11}$$

where $\sigma_{ij}$ represents the stress values at point i and in direction j and $u^*_{ijk}$ as well as $p^*_{ijk}$ represents the fundamental solutions of displacement and traction components, respectively, which can be determined by adding full-plane fundamental solutions to the complementary part [23].

### 2.3. Discretizing BIE

After discretizing the boundaries of the body with N quadratic elements, the discretized form of BIE can be shown as follows:

$$c_{ij} u^i = \sum_{k=1}^{N} \int_{\Gamma_k} u^*_{ij} p_j \, d\Gamma_k - \sum_{k=1}^{N} \int_{\Gamma_k} p^*_{ij} u_j \, d\Gamma_k \tag{12}$$

In this expression, $\Gamma_k$ denotes the boundary of element k. The matrix form of the above equation can be shown as follows:

$$H \times U = G \times P \tag{13}$$

where U and P denote the boundary displacement and traction vectors and H and G are the matrixes that can be calculated using the following equations:

$$H_{ij} = \int_\Gamma p^*_{ij} \, d\Gamma \tag{14}$$

$$G_{ij} = \int_\Gamma u^*_{ij} \, d\Gamma \tag{15}$$

### 2.4. Modeling

To model a two-layer soil domain that includes a lined cavity, the problem can be divided into three distinct parts. The first part ($\Omega_1$) consists of a soil surface layer, the second part ($\Omega_2$) contains a semi-infinite domain as the second soil layer and outer boundary of cavity, and the third part ($\Omega_3$) contains only the outer and inner pipe boundaries as a finite body (Fig. 2).

The matrix form of BIEs for $\Omega_1$ can be written as follows:

$$\begin{bmatrix} H_{11} & H_{12} \end{bmatrix} \begin{bmatrix} u_{11} \\ u_{12} \end{bmatrix} = \begin{bmatrix} G_{11} & G_{12} \end{bmatrix} \begin{bmatrix} p_{11} \\ p_{12} \end{bmatrix} \tag{16}$$

where ($H_{11}$ and $G_{11}$) and ($H_{12}$ and $G_{12}$) represent the matrix form of BIE for ground surface boundary ($\Gamma_{11}$) and two-layer interface boundary ($\Gamma_{12}$), respectively. The matrix form for the second part ($\Omega_2$) can be written as follows:

$$\begin{bmatrix} H_{21} & H_{23} \end{bmatrix} \begin{bmatrix} u_{21} \\ u_{23} \end{bmatrix} = \begin{bmatrix} G_{21} & G_{23} \end{bmatrix} \begin{bmatrix} p_{21} \\ p_{23} \end{bmatrix} \tag{17}$$

where ($H_{21}$ and $G_{21}$) and ($H_{23}$ and $G_{23}$) represent the matrix form of BIE for the interface boundary ($\Gamma_{21}$) and pipe outer boundary ($\Gamma_{23}$), respectively; finally, for the third part ($\Omega_3$) matrix, equations can be easily written as follows:

$$\begin{bmatrix} H_{32} & H_{33} \end{bmatrix} \begin{bmatrix} u_{32} \\ u_{33} \end{bmatrix} = \begin{bmatrix} G_{32} & G_{33} \end{bmatrix} \begin{bmatrix} p_{32} \\ p_{33} \end{bmatrix} \tag{18}$$

where ($H_{32}$ and $G_{32}$) and ($H_{33}$ and $G_{33}$) represent the matrix form of BIE for pipe outer boundary ($\Gamma_{32}$) and pipe inner boundary ($\Gamma_{33}$), respectively. For extracting the coupled matrix, it is necessary to apply stress continuity and displacement compatibility conditions for interface boundaries. In this problem, there are two interface boundaries between soil layers ($\Gamma_{12}$) and pipe-soil contact zone ($\Gamma_{23}$). Continuity and compatibility conditions for the interface boundaries can be mathematically written as follows:

$$\begin{cases} u_{12} = u_{21} \\ p_{12} + p_{21} = 0 \end{cases} \tag{19}$$

$$\begin{cases} u_{23} = u_{32} \\ p_{23} + p_{32} = p_g \end{cases} \tag{20}$$

In this expression, $P_g$ denotes the effect of gravitational stresses on pipe body. After combining Eqs. (14)–(18), the coupled matrix for analyzing a two-layer soil including a buried pipe can be easily extracted as follows:

$$\begin{bmatrix} H_{11} & H_{12} & 0 & 0 \\ 0 & H_{21} & H_{23} & 0 \\ 0 & 0 & H_{32} & H_{33} \end{bmatrix} \begin{bmatrix} u_{11} \\ u_{12} \\ u_{23} \\ u_{33} \end{bmatrix} = \begin{bmatrix} G_{11} & G_{12} & 0 & 0 \\ 0 & -G_{21} & G_{23} & 0 \\ 0 & 0 & -G_{32} & G_{33} \end{bmatrix} \begin{bmatrix} p_{11} \\ p_{12} \\ p_{23} \\ p_{33} \end{bmatrix} + \begin{bmatrix} 0 & 0 & 0 \\ 0 & 0 & 0 \\ 0 & 0 & G_{32} \end{bmatrix} \begin{bmatrix} 0 \\ 0 \\ p_g \end{bmatrix} \tag{21}$$

Finally, by applying external boundary conditions to the free boundaries ($\Gamma_{11}$ and $\Gamma_{33}$), the soluble form of Eq. (21) can be obtained as follows:

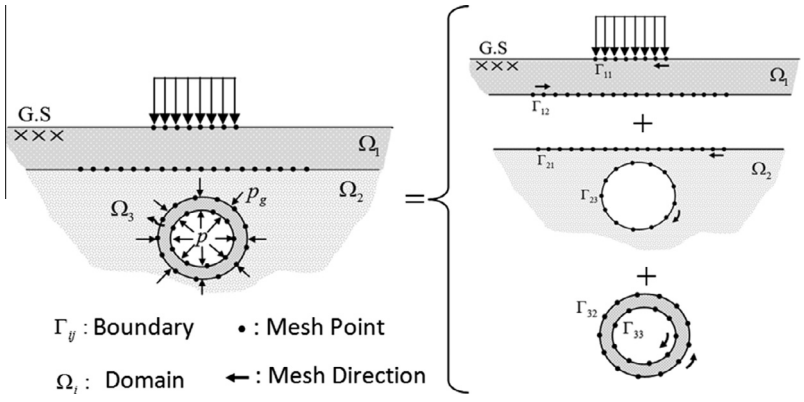


**Fig. 2.** Modeling a pipe embedded in two-layer soil using half-plane BEM.

$$\underbrace{\begin{bmatrix} H_{11} & H_{12} & 0 & 0 & -G_{12} & 0 \\ 0 & H_{21} & H_{23} & 0 & G_{21} & -G_{23} \\ 0 & 0 & H_{32} & H_{33} & 0 & G_{32} \end{bmatrix}}_{A} \underbrace{\begin{bmatrix} u_{11} \\ u_{12} \\ u_{23} \\ u_{33} \\ p_{12} \\ p_{23} \end{bmatrix}}_{X} = \underbrace{\begin{bmatrix} G_{11} & 0 \\ 0 & 0 \\ 0 & G_{33} \end{bmatrix} \begin{bmatrix} p_{11} \\ p_{33} \end{bmatrix} + \begin{bmatrix} 0 & 0 \\ 0 & 0 \\ 0 & G_{32} \end{bmatrix} \begin{bmatrix} 0 \\ p_g \end{bmatrix}}_{F} \quad (22)$$

where

$$AX = F \quad (23)$$

In the above equation, X represents the unknown boundary values, A is the coefficients' squared matrix corresponding to unknown values, and F represents a vector that contains known values.

### 2.5. Verification

In order to analyze a two-layer soil including a circular pipe, a computer algorithm was developed based on the above formulation using MATLAB software [17]. This algorithm can analyze the effects of combined surcharge and pipe pressure on soil stress distributions; moreover, it can present stress and displacement values for any internal point. Due to the lack of analytical solutions for the model of shallow pipes in layered soils, analytical results of Jeffery [22], Jaeger [21], Poulos and Davis [15] as well as Li and Wang [20] were used for verifying this algorithm.

Jeffrey [22] presented an analytical response for ground surface horizontal stresses due to a pressure circular unlined cavity, embedded in a homogenous semi-infinite domain. In this regard, for the first layer, second layer, and pipe body was introduced a similar material properties. Fig. 3 shows the half-plane BEM responses compared with Jeffrey's analytical solutions [22]. As can be seen in figure, a good match between the analytical and numerical results can be observed. It should be noted that, for solving this model using present method, only 100 quadratic elements were used.

Poulos and Davis [15] obtained an analytical response for vertical stresses in two-layer domains. In their study, the second layer was considered as rigid and a uniform load affected on the ground surface. For introducing this model into the present study, elastic module of the second layer was selected as a large amount (about 200 GPa). Also, to eliminate the effect of cavity, the radius of pipe was assumed as an insignificant number (1 cm) and the depth was a large number (about 50 m) compared to other parameters. Results of the comparison are shown in Fig. 4; it can be seen that there was good agreement between the analytical and numerical responses.

In the third example, a lined cavity in an infinite domain was studied. Jaeger [21] was able to present an analytical response for radial stress distribution near the lined cavities that were constructed in deep soil. To achieve this purpose, in the present study, the depth of pipe was assumed to be a large number (200 m). Then, the radial stress in the pipe wall was calculated and compared with Jaeger's analytical solution [21] in Fig. 5. As can be seen in the figure, there was good agreement between the analytical and numerical results.

Shallow lined cavities under internal and ground surface pressures have been studied by Li and Wang [20]. They presented analytical solutions for radial stress distribution around a lined

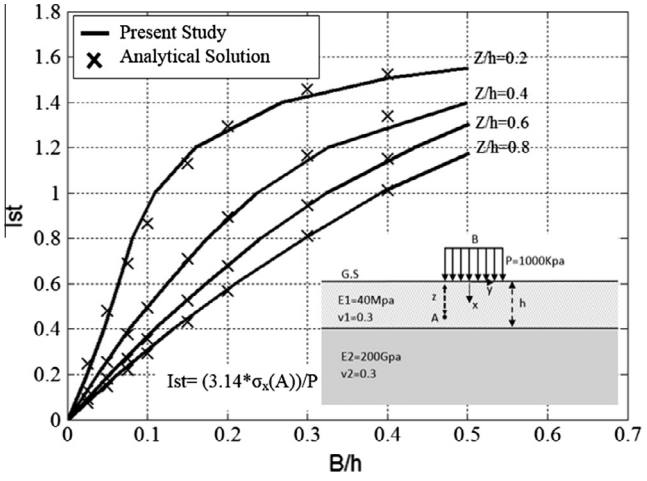


**Fig. 4.** Comparison of an analytical response [15] and the present study for a two-layer domain with rigid half-plane.

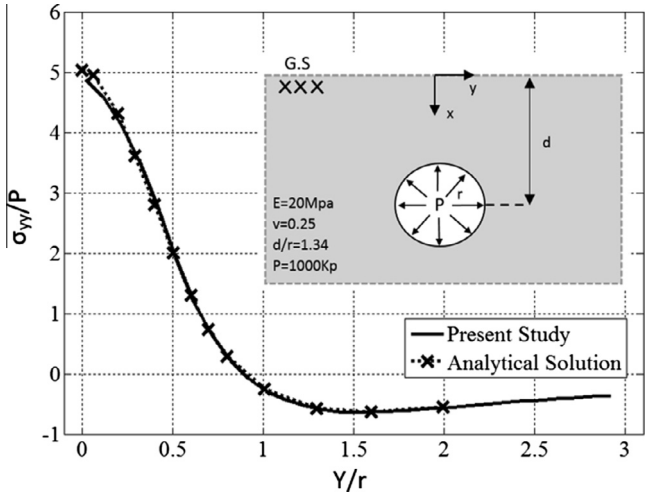


**Fig. 3.** Comparison of an analytical response [22] and the present study for a circular cavity embedded in a single homogeneous layer.

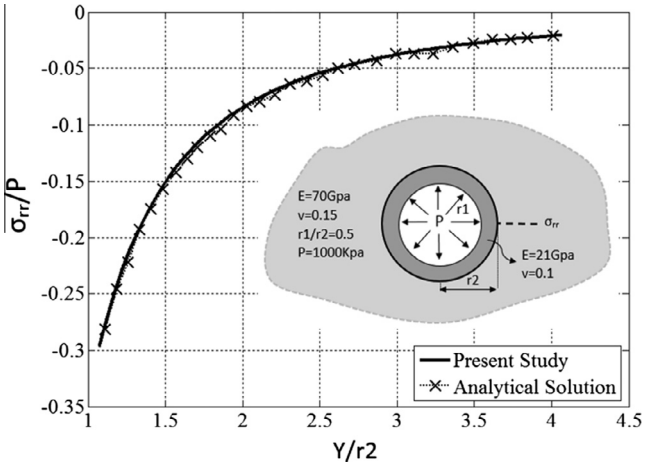


**Fig. 5.** Comparison of an analytical response [21] and the present study for a deep lined tunnel.

circular cavity. For comparing these results with the half-plane BEM solution, the same problem was modeled. The results are presented in Fig. 6 for radial stresses. As can be seen in the figure, there was good agreement between the analytical and numerical results.

### 2.6. Parametric study

In this section, in a parametric study, a circular pressure pipe buried in the second layer of a two-layer soil was modeled and the effects of pipe depth on the ground surface displacements as well as the stress distribution of soil were evaluated. Material properties of the soil layers and pipe body are considered in Fig. 7. Soil's first layer was assumed to be soft clay with $\gamma_1 = 15$ kN/m$^3$, $E_1 = 20$ MPa, and $\nu_1 = 0.25$ and its thickness was assumed h = 2 m. The second layer's material was assumed to be well grained sand with $\gamma_2 = 19$ kN/m$^3$, $E_2 = 40$ MPa, and $\nu_2 = 0.3$ and the material of the pipe body was assumed to be cast iron with $E_3 = 165$ GPa and $\nu_3 = 0.22$. The pipe's inner radius was r = 0.5 m and its thickness was t = 1 mm. For modeling the pipe's internal pressure, a uniform pressure (P = 1000 kPa) was applied to the inner pipe boundary. Also, a uniform load ($P_s = 1000$ kPa) was applied on free boundary of model (Fig. 7) and it's width was assumed to be B = 6 m. For achieving good accuracy, the pipe boundaries were totally discretized using 60 quadratic elements, and the interface boundary between soil layers was discretized using 50 quadratic elements. It should be noted that, according to Fig. 7, for modeling the effect of gravitational pressure, the external load of $P_g$ was applied to the outer pipe boundary as follows:

$$P_g = \gamma_1 h + \gamma_2 (d - h) \tag{24}$$

where $\gamma_1$ and $\gamma_2$ are the unit weights of the first and second soil layers, h is the thickness of soil's first layer, and d is the pipe depth (Fig. 7).

Surface displacements in the presence of pipe lines and surface loads are one of the interesting topics for geotechnical engineers. In big cities pipes and lined tunnels are the most common geotechnical structures. These structures can change the stress distributions in soil body and cause different type of soil surface displacements. In this study, the surface displacements were studied in two cases. In first case, it was assumed that the pipe is embedded in the second layer and it has no internal pressure (P = 0). Also, for modeling the effects of a ground structure, a surface load ($P_s = 1000$ kPa) is applied on the ground surface (Fig. 7). Figs. 8–10 show the surface

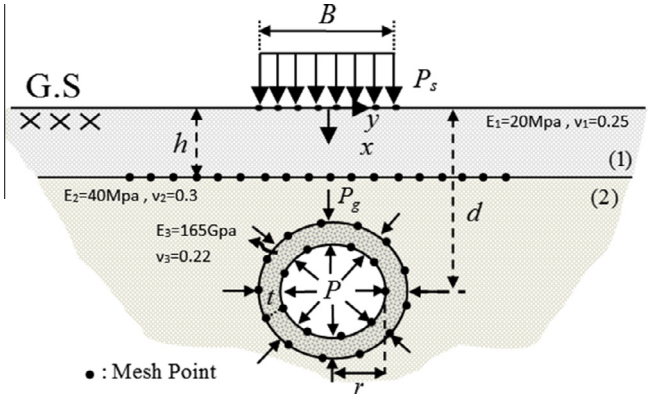


**Fig. 7.** Schematic representation for this study.

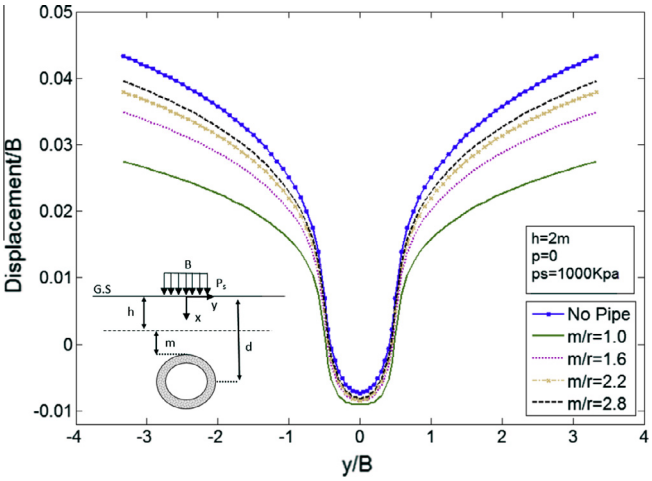


**Fig. 8.** Ground surface displacements for the two-layer soil in the presence of a pressure pipe and surface load (h = 2 m, r = 0.5 m).

displacements for this case. It is obvious that there are two type of displacements on the ground surface in this case: the settlement and swelling, which its magnitudes are related to the thickness of first layer as well as pipe depth and geometrical properties respectively. When the thickness of the surface layer increases, the settlements and swelling increase on the ground. Generally,

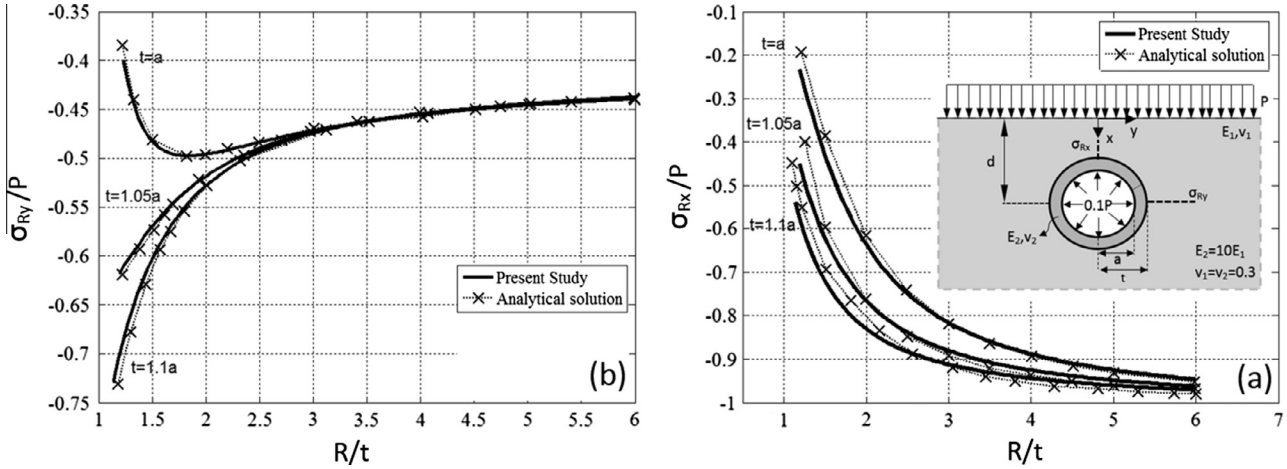


**Fig. 6.** Comparison of an analytical response [20] and the present study for radial stresses near shallow lined tunnel (R = radial distance from center of tunnel).

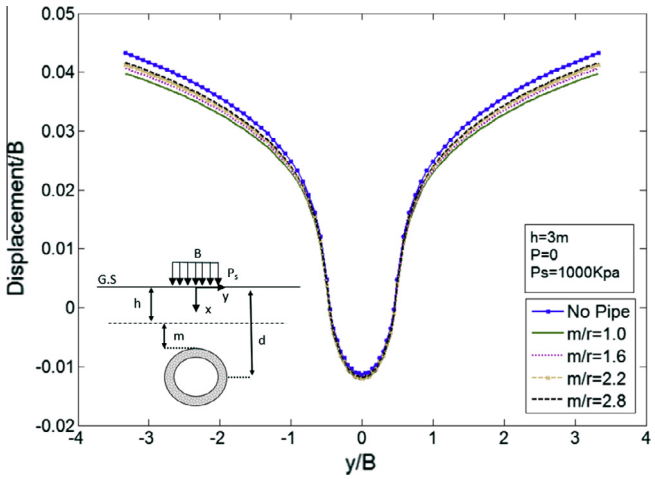


**Fig. 9.** Ground surface displacements for the two-layer soil in the presence of a pressure pipe and surface load (h = 3 m, r = 0.5 m).

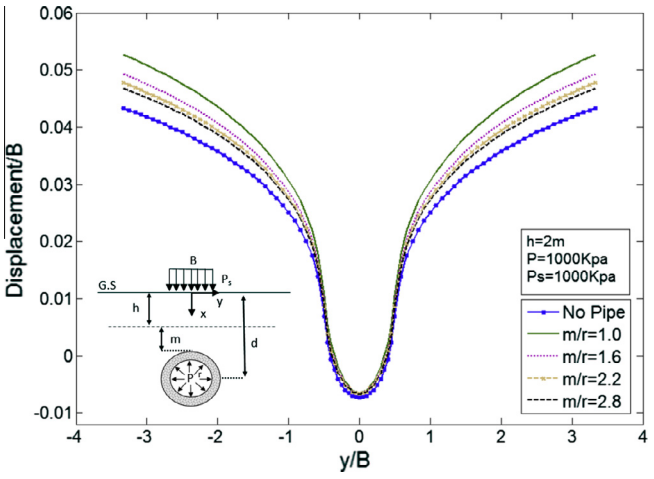


**Fig. 11.** Ground surface displacements for the two-layer soil in the presence of a pressure pipe and surface load (h = 2 m, r = 0.5 m).

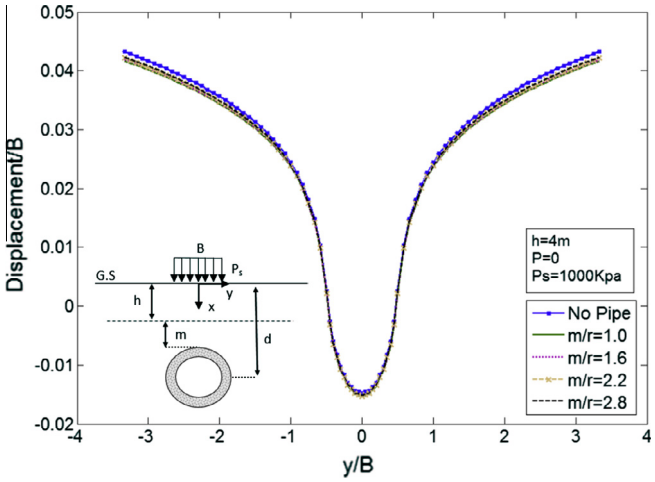


**Fig. 10.** Ground surface displacements for the two-layer soil in the presence of a pressure pipe and surface load (h = 4 m, r = 0.5 m).

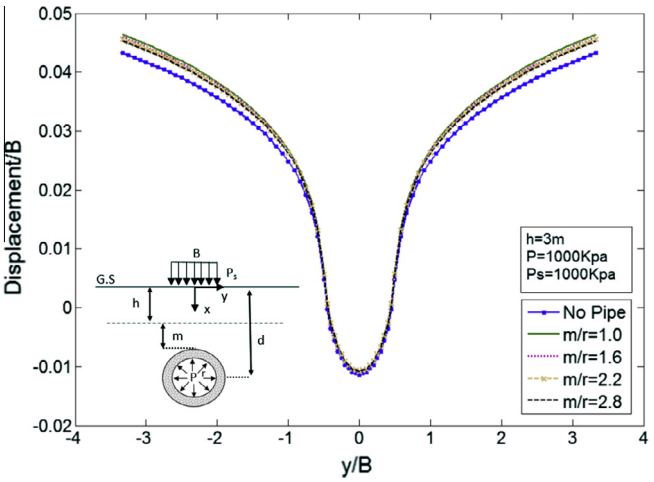


**Fig. 12.** Ground surface displacements for the two-layer soil in the presence of a pressure pipe and surface load (h = 3 m, r = 0.5 m).

the depth of pipe has an inverse ratio with the magnitude of surface settlements, i.e. the maximum settlements occurs when the pipe is near the ground surface.

In second case, surface load and pipe pressure was assumed as Ps = 1000 kPa and P = 1000 kPa, respectively. The pipe pressure was difference between this case and the former. Figs. 11–13 show the ground surface displacements for h = 2 m, 3 m and 4 m, respectively. As can be seen, according to the previous case, when the thickness of the first layer is equal to h = 4 m, maximum settlements occurs; however when the thickness is equal to h = 2 m, the maximum swelling takes place. This is notable; when the thickness of first layer is greater than 3 m, the relation between surface displacements and pipe depth diminishes slowly and all carves show the same magnitude for displacements.

Stress distribution near the pipe due to fluid pressure is another interesting topic for the engineers. When constructing geotechnical buildings, the patterns of stress distribution can help to obtain good stability predictions. The stress values and its patterns around the pipe change by increasing the pipe depth. For observing these changes, radial stresses at right side of the pipe (x = d) was plotted in Figs. 14–16 for h = 2 m, 3 m and 4 m, respectively. Mate-

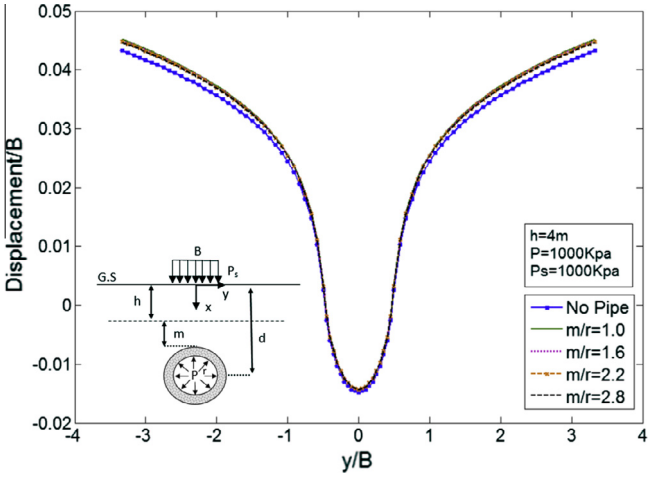


**Fig. 13.** Ground surface displacements for the two-layer soil in the presence of a pressure pipe and surface load (h = 4 m, r = 0.5 m).

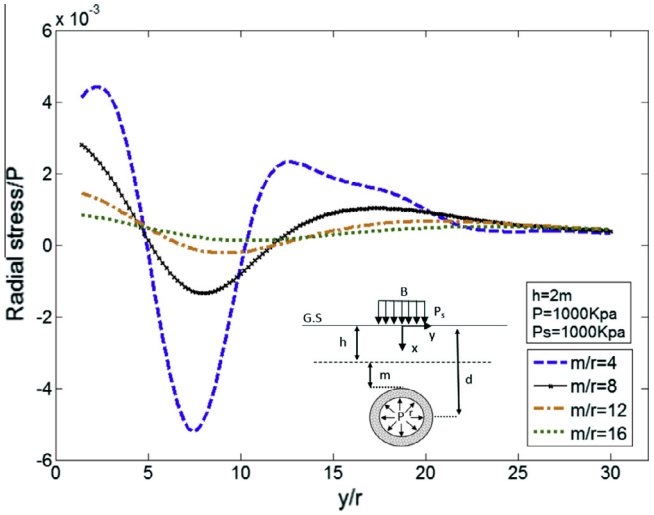


**Fig. 14.** Radial stresses near the pipe for the different depths (h = 2 m, B = 6 m).

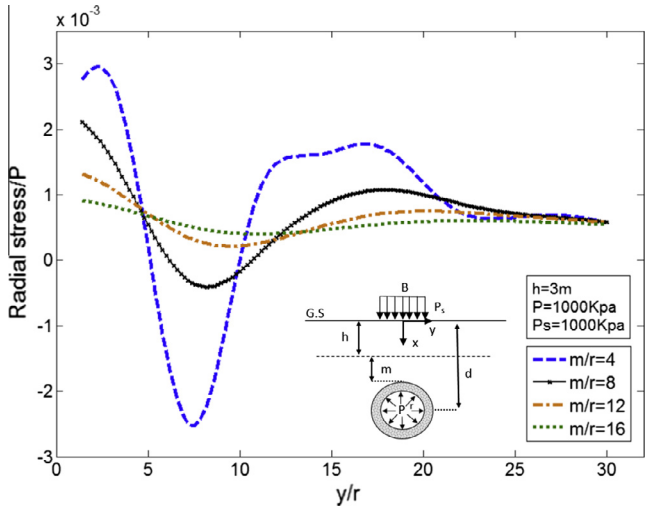


**Fig. 15.** Radial stresses near the pipe for the different depths (h = 3 m, B = 6 m).

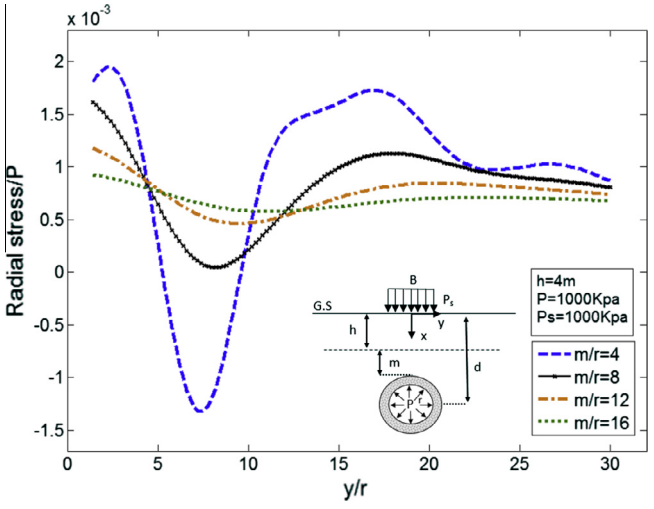


**Fig. 16.** Radial stresses near the pipe for the different depths (h = 4 m, B = 6 m).

rial and geometrical properties of this study are the same as used in previous example. Surface load pressure and internal pressure of pipe is equal to $P_s$ = 1000 kPa and P = 1000 kPa respectively.

As can be seen, for a fixed h, by increasing the pipe depth, the radial stresses decreases effectively near the pipe. When the pipe is near the interface i.e. m is equal to 4r, radial stresses have a great peak and their magnitude decreases rapidly with increasing m. First layer thickness is another effective variable which change the shape and magnitude of radial stresses near the pipe. When the thickness of shallow layer increases, the magnitude of radial stresses decrease because of increasing of pipe depth. But, when the pipe is near the interface of soil layers, the shape of radial stress are the different.

In general, it can be concluded that the half-plane BEM has good capability for modeling underground geotechnical structures and it can give accurate responses when a pipe model embedded in layered soil is considered.

## 3. Conclusions

In this paper, formulation and application of half-plane BEM for analyzing pressure pipes embedded in the layered soils were presented. After preparing a computer algorithm and carrying out necessary verifications, a pressure pipe buried in two-layer soil was analyzed. Studies showed that the accuracy of half-plane BEM for analyzing semi-infinite domains was quite suitable. The number of elements used for modeling an embedded cavity in layered media was reduced by 50% compared with full-plane BEM [11,12]. Because this method did not require closing the boundaries in the far-field of interested area and discretizing only some constrained boundaries, it can increase the accuracy of results compared with other methods. In the parametric study, the simplicity of half-plane BEM was demonstrated for modeling embedded pressure pipes and effects of pipe depth on soil stress distribution were evaluated by presenting some stress patterns. Half-plane BEM can be a good alternative to other methods for modeling geotechnical subsurface buildings.

Whereas the examples presented in this paper showed some capabilities of the half-plane BEM, it is obvious that the method had also some important limitations. Stress analysis of multi-phase mediums as well as undrained soils with the half-plane BEM was not so straightforward. Besides, due to the complexity of the half-plane fundamental solutions, they could not be simply extended to important cases such as anisotropic and nonlinear media. This kind of problems could be solved more efficiently by the FEM. Combining the half-plane BEM with the FEM and using the advantages of each method in its place seems to be another efficient way which should be experienced in the future.

## References

[1] Augarde CE, Burd HJ. Three-dimensional finite element analysis of lined tunnels. Int J Numer Anal Meth Geomech 2001;25(3):243–62.
[2] Brebbia CA, Dominguez J. Boundary element introduction course. 2nd ed. Southampton Computational Mechanics Publications; 1992.
[3] Crouch SL, Starfield AM. Boundary element method in solid mechanics. Dept of Civil and Mineral Engineering, University of Minnesota; 1983.
[4] Cheng Alexander HD, Cheng Daisy T. Heritage and early history of the boundary element method. Eng Anal Boundary Elem 2005;29:268–302.
[5] Duffy DG. Green's function with applications. Boca Raton (FL): Chapman & Hall/CRC Press; 2001.
[6] Dumir PC, Mehta AK. Boundary element solution for elastic orthotropic half-plane problems. J Comput Struct 1987;26:431–8.
[7] Dong CY, Lo SH. Boundary element analysis of an elastic half-plane containing nanoinhomogeneities. J Comput Mater Sci 2013;73:33–40.
[8] Dong CY, Lo SH, Cheung YK. Numerical solution for elastic half-plane inclusion problems by different integral equation approaches. Eng Anal Boundary Elem 2004;28:123–30.
[9] Katsikadelis JT. Boundary element theory and applications. 1st ed. National Technical University of Athens; 2002.

[10] Pan Emian, Chen Chao-Shi, Amadei Bemard. A BEM formulation for anisotropic half-plane problems. Eng Anal Boundary Elem 1997;20(3):185–95.
[11] Panji M, Marnani J Asgari, Tavousi Tafreshi Sh. Evaluation of effective parameters on the underground tunnel stability using BEM. J Struct Eng Geotech 2011;1(2):29–37.
[12] Panji M, Koohsari H, Adampira M, Alielahi H, Marnani J Asgari. Analyzing stability of shallow tunnels subjected to eccentric loads by a BEM approach. J Rock Mech Geotech Eng 2016;8:480–8.
[13] Panji M, Kamalian M, Marnani J Asgari, Jafari MK. Transient analysis of wave propagations problems by half-plane BEM. Geophys J Int 2013;194:1849–65.
[14] Panji M, Kamalian M, Marnani J Asgari, Jafari MK. Analysing seismic convex topographies by a half-plane time-domain BEM. Geophys J Int 2014;197 (1):591–607.
[15] Poulos HG, Davis EH. Elastic solutions for soil and rock mechanics. Center for Geotechnical Research, John Wiley & Sons Inc; 1991. ISBN 0471695653.
[16] Mindlin RD. Stress distribution around a hole near the edge of a plate under tension. Proc Soc Exp Stress Anal 1948;2:56–68.
[17] Matlab, Primer. The math works Inc, 3 Apple Hill Drive Natick, MA 01760-2098; 2014. www.mathworks.com.
[18] Mroueh H, Shahrour I. Three-dimensional finite element analysis of the interaction between tunneling and pile foundations. Int J Numer Anal Meth Geomech 2002;26(3):217–30.
[19] Garner Cyrus D, Coffman Richard A. Subway tunnel design using a ground surface settlement profile to characterize an acceptable configuration. Tunn Undergr Space Technol 2013;35:219–26.
[20] Li SC, Wang MB. Elastic analysis of stress-displacement field for a lined circular tunnel at great depth due to ground loads and internal pressure. J Tunn Undergr Space Technol 2008;23:609–17.
[21] Jaeger JC. Elasticity fracture and flow with engineering and geological applications. 2nd ed. London: Methuen; 1964.
[22] Jeffery GB. Plane stress and plane strain in bipolar coordinates. Philos Trans R Soc Math Phys Eng Sci 1920;221:265–93.
[23] Telles JCF, Brebbia CA. Boundary element solution for half-plane problems. Int J Solids Struct 1980;12:1149–58.
[24] Xiao B, Carter JP. Boundary element analysis of anisotropic rock masses. Eng Anal Boundary Elem 1993;11:293–303.
[25] Wu R, Xu JH, Li C, Wang ZL, Qin S. Stress distribution on mine roof with the boundary element method. Eng Anal Boundary Elem 2015;50:39–46.
[26] Ye GW, Sawada T. Some numerical properties of boundary element analysis using half-plane fundamental solutions in 2-d elastostatics. J Comput Mech 1989;4:161–4.
[27] Yang L, Sterling RL. Back analysis of rock tunnel using boundary element method. J Geotech Eng 1989;115(8):1163–9.